

## Numerical Simulation of High Lift Trap Wing Using STAR-CCM+

Prashanth S. Shankara, Deryl Snyder  
CD-adapco

# Outline

- ⑤ **Motivation**
- ⑤ **Cases overview**
- ⑤ **Solver & boundary conditions**
- ⑤ **Mesh**
- ⑤ **Results – Config 1 without brackets**
- ⑤ **Results – Config 1 with brackets**
- ⑤ **Conclusion**

# Motivation



- ⊗ Investigation of STAR-CCM+ high lift aerodynamics prediction capability
- ⊗ Model high-lift physics in a manner well-suited for industrial design use
  - Automated and unstructured polyhedral mesh
- ⊗ Performance of  $\gamma$ - $Re_{\theta}$  transition model

# High Lift Aerodynamics

## ⊗ Aerodynamics of 3D swept wings in high-lift configurations is very complex

- Separation
- Unsteadiness
- Confluent boundary layers
- Transition
- Vortical flow

## ⊗ AIAA HiLiftWS1 (2010)

- Assess capabilities of current-generation codes
  - Meshing
  - Numerics
  - Turbulence Modeling
  - High-performance computing



# NASA 'Trap Wing' model

⊗ Tested in 1998-1999, 2002-2003  
at NASA Langley and NASA  
Ames wind tunnels

⊗  $Re \sim 4.6 \text{ M}$

- No turbulent trips – transition is a factor

⊗ **Data collected**

- Aerodynamic forces/moments
- Pressure distributions
- Transition location
- Acoustics



Trap wing in NASA LaRC 14x22 WT

# STAR-CCM+



- ⊗ STAR-CCM+ v6.06.011
  - Mesh, Solve, Post-process
- ⊗ Density-based coupled solver
  - Low Mach number preconditioning
  - Algebraic Multi-Grid (AMG) acceleration
- ⊗ 2<sup>nd</sup>-order spatial discretization
- ⊗ Steady-state RANS equations
  - Implicit pseudo time-marching scheme
- ⊗ SST (Menter) k- $\omega$  turbulence model
  - Integrated to the wall
- ⊗  **$\gamma$ -Re $_{\theta}$  Transition Model**
- ⊗ **Arbitrary unstructured polyhedral mesh**

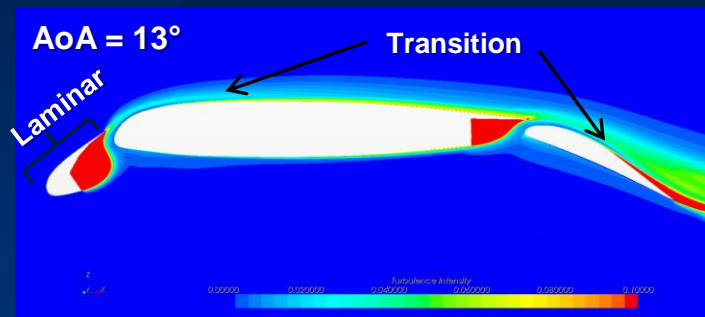
# $\gamma$ - $Re_{\theta}$ Transition Model

## ⊗ Without transition modeling

- Lift coefficients generally under-predicted
- Late stall prediction

## ⊗ Predicts laminar-turbulent transition in the boundary layer

- Correlation-based model formulated for unstructured CFD codes
  - Uses locally computed vorticity-based  $Re$
- In conjunction with SST  $k$ - $\omega$  turbulence model
- Models transport of Momentum Thickness  $Re$  ( $Re_{\theta}$ ) and Intermittency ( $\gamma$ )
- Turbulence Intensity and Intermittency as transition identification parameters



# Cases

## ⊗ Case 1 – Configuration 1, No brackets

- Slats at  $30^\circ$  and flap at  $25^\circ$
- Three mesh sizes (coarse, medium, fine)
- Angles of attack varying from  $6^\circ$  to  $37^\circ$

## ⊗ Case 2 – Configuration 1 with brackets

- $\alpha$  –  $6^\circ$ ,  $13^\circ$ ,  $21^\circ$ ,  $23^\circ$ ,  $25^\circ$ ,  $27^\circ$ ,  $28^\circ$
- Medium mesh (No grid convergence study)



# Boundary conditions

## ⊗ No-slip wall conditions

- No transition location specified

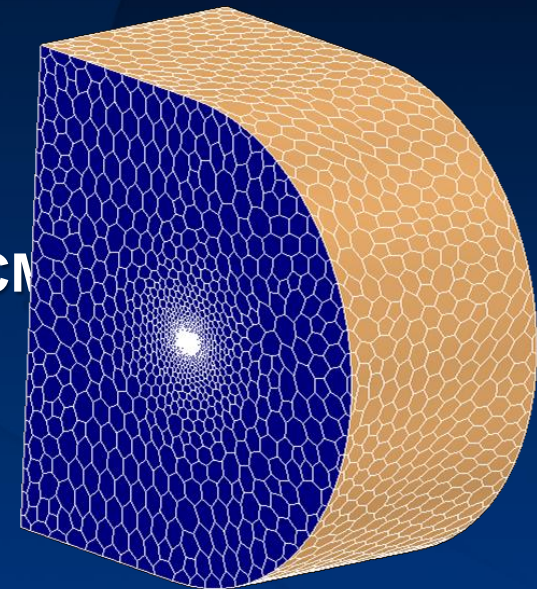
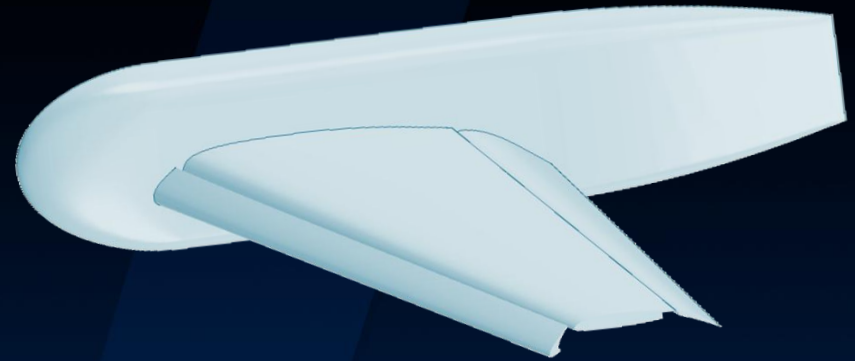
## ⊗ Symmetry plane

## ⊗ Freestream

- Mach 0.2
- $T = 520R$
- $P = 1 \text{ atm}$
- $Re = 4.3M$  based on MAC
- $\alpha = 6, 13, 21, 28, 32, 34, 35, 36, 37 \text{ deg}$
- Turbulence intensity =  $7.5e-4$  (WT data)

## ⊗ Farfield boundaries created in STAR-CCM+

- Extends 100MAC in all directions



# Computational Mesh Overview



## ⊗ Polyhedral unstructured mesh

- Three different mesh sizes for grid refinement study
- Wide range of angles of attack on a single mesh
- Arbitrary geometry shapes used for focused refinement

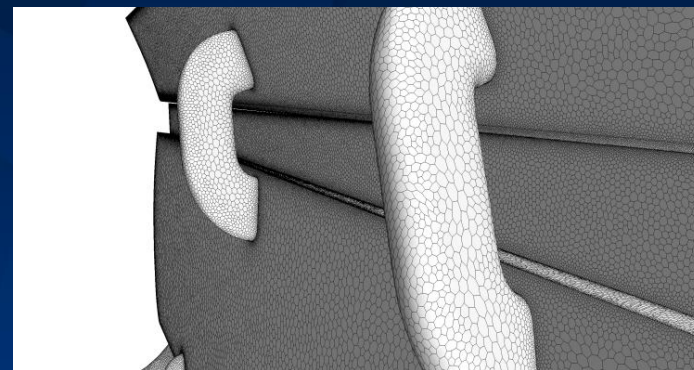
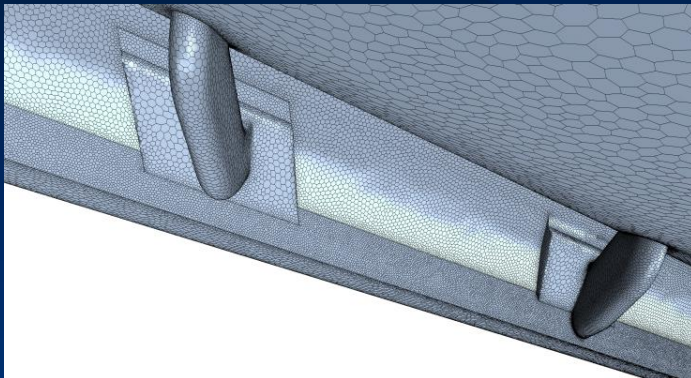
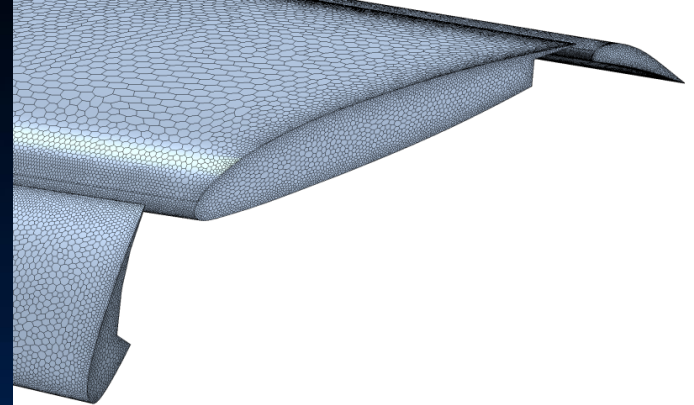
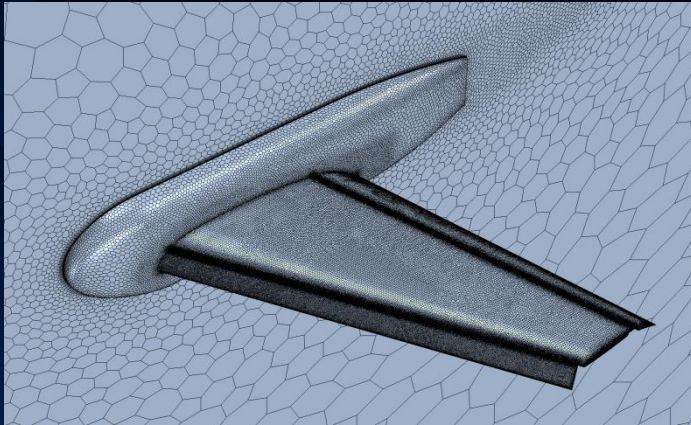
## ⊗ 25 prism Layers

- First cell  $y^+ < 1.0$

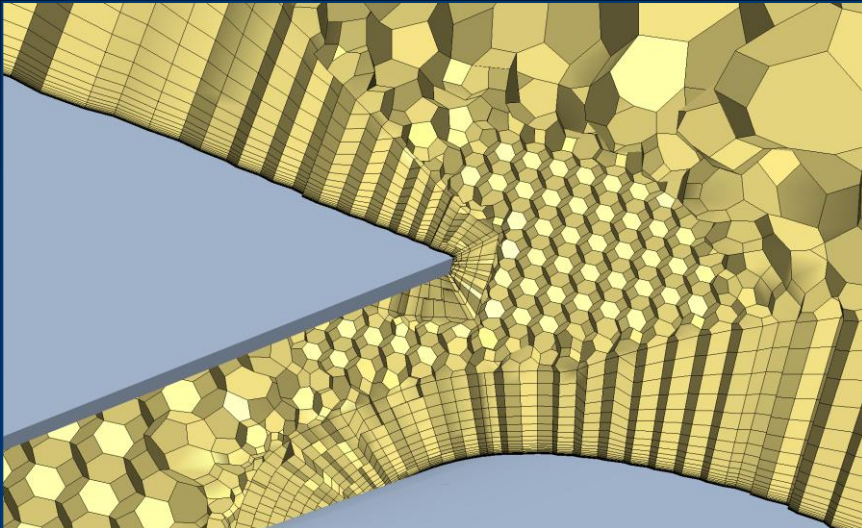
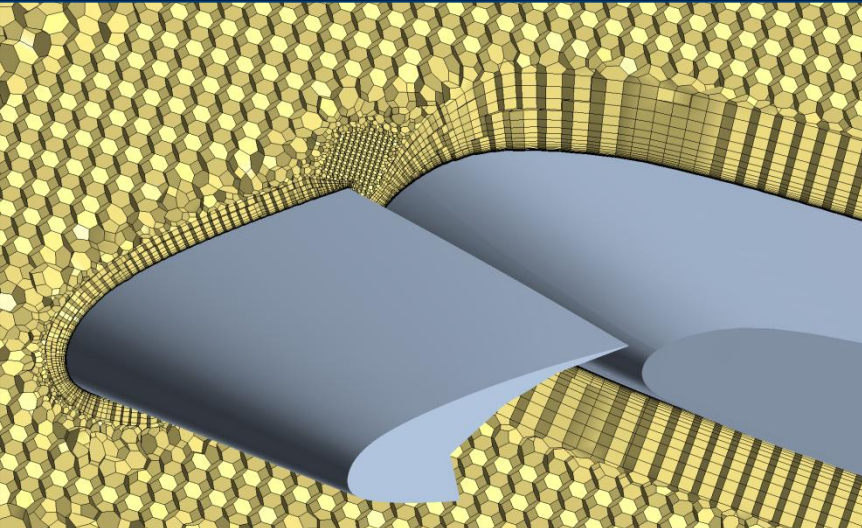
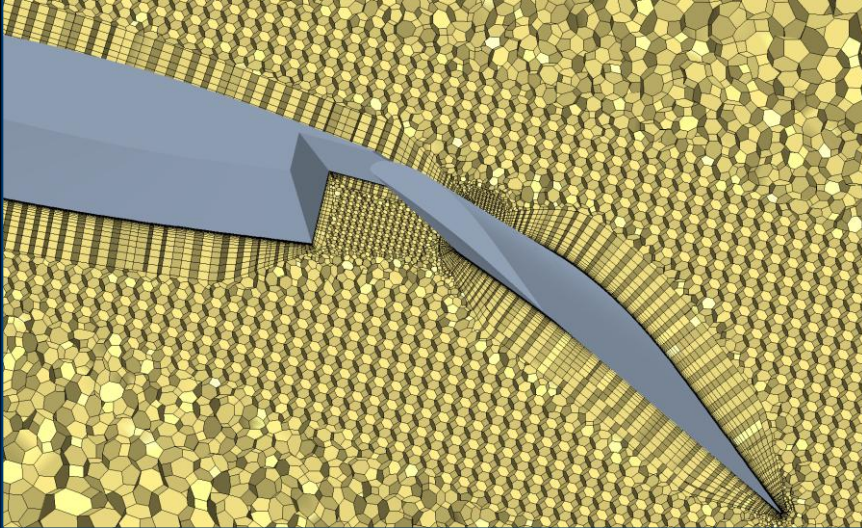
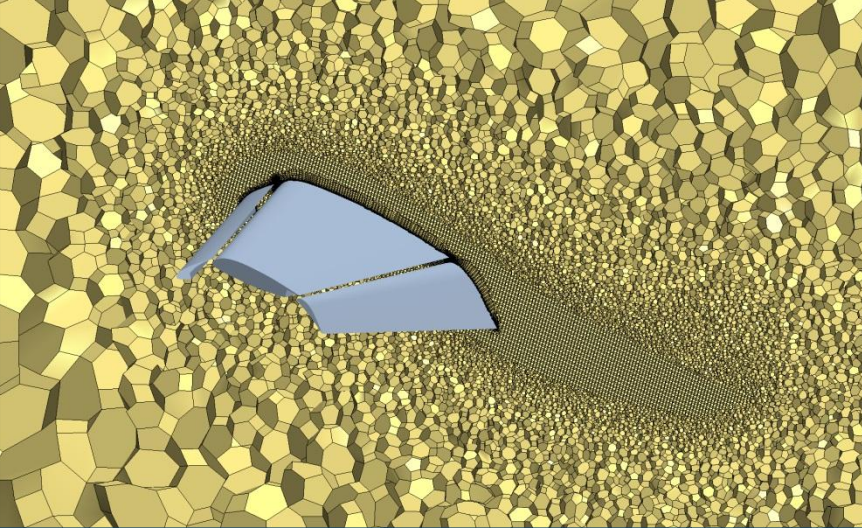
Parameter	Coarse	Medium	Fine	Med. (brackets)
No. of cells	10M	22M	34M	20M
No. of surface faces	46M	112M	184M	
Target prism layer height	$0.032C_{ref}$	$0.032C_{ref}$	$0.032C_{ref}$	$0.032C_{ref}$
Cells across trailing edge	6	10	12	10
Near-wall cell height (m)	5e-6	3.3e-6	1e-6	3.3e-6

# Mesh – Surface

⊕ Surface faces refined on curvature, sharp edges, near tip



# Mesh – Volume

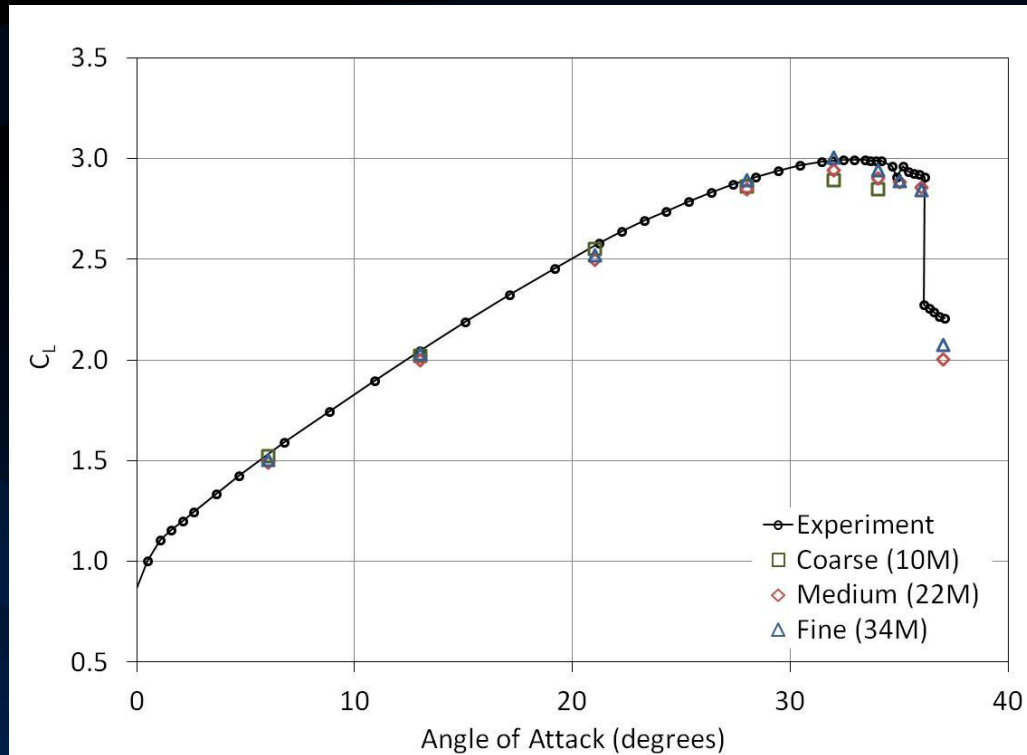


# Solution Strategy

## ⊗ Solution strategy

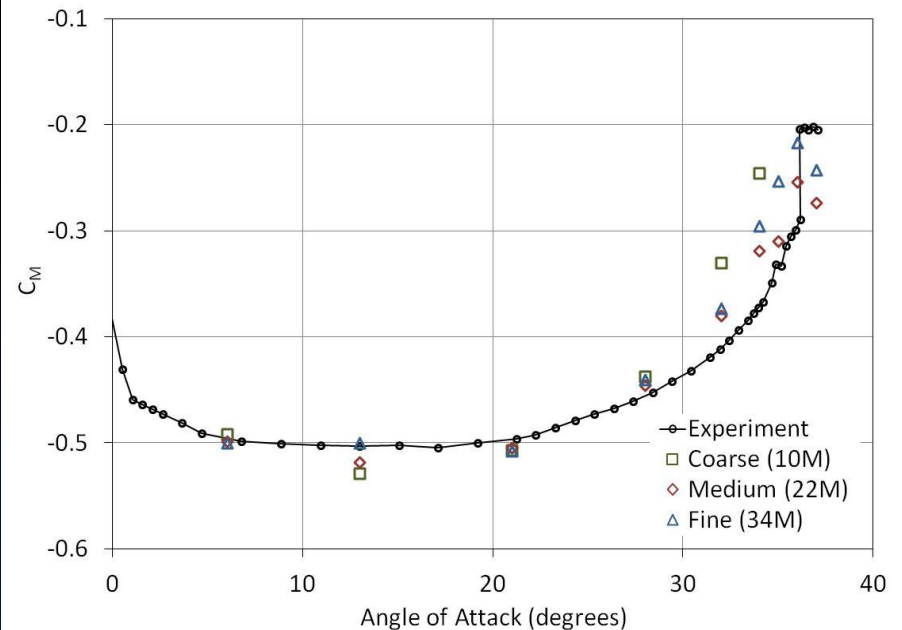
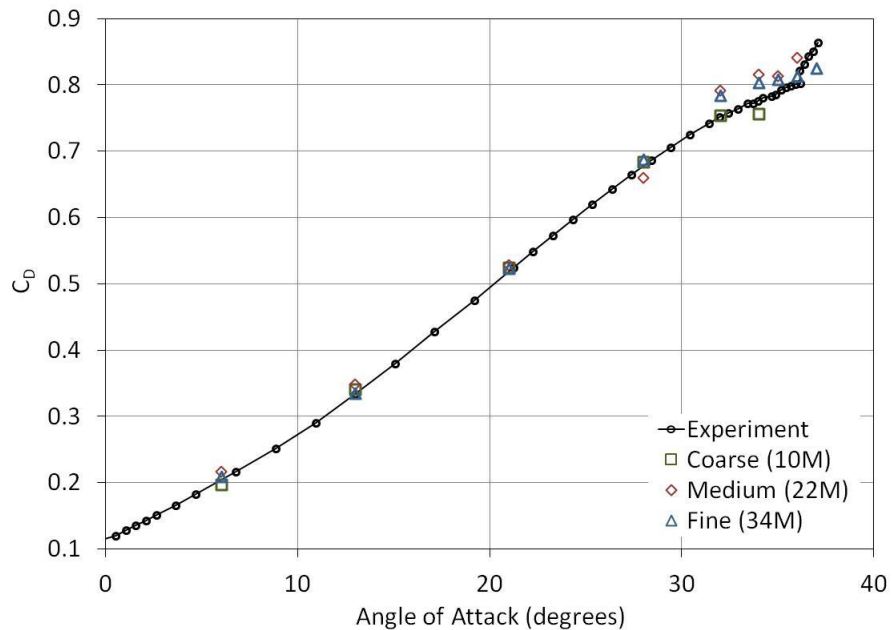
- For  $\alpha = 6^\circ$  to  $28^\circ$ 
  - Initialized via grid-sequencing technique
  - Obtain a stable solution without transition model
  - Introduce transition model
- For  $\alpha = 32^\circ$  &  $34^\circ$ 
  - Initialized from previous angle of attack
  - Obtain a stable solution without transition model
  - Introduce transition model
- For  $\alpha = 35^\circ$ ,  $36^\circ$  &  $37^\circ$ 
  - Initialized from previous angle of attack

# Lift Coefficient



- ⊗ Both medium and fine mesh predicts post-stall region well
- ⊗ Results improve with mesh refinement
- ⊗  $C_{LMax}$  deviation
  - Coarse mesh: 3.3% (low)
  - Medium mesh: 1.6% (low)
  - Fine mesh: 0.4% (high)

# Drag & Moment Coefficient



## ⊗ Drag

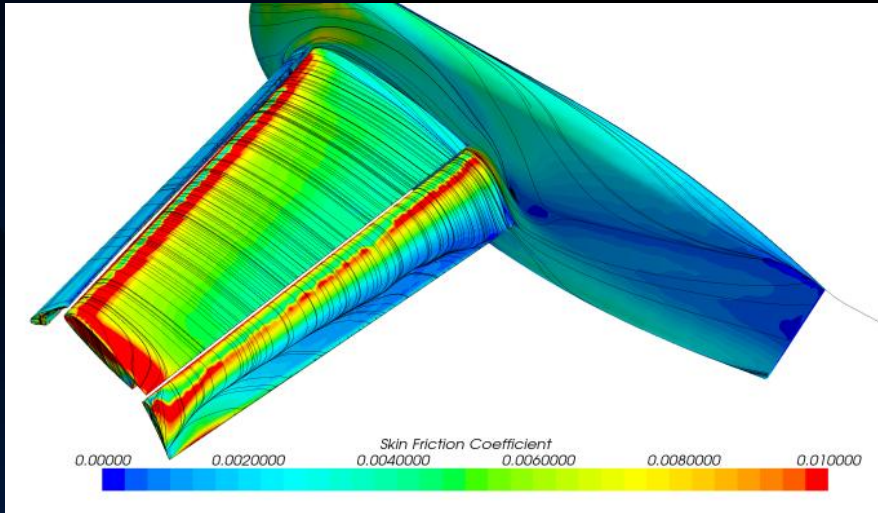
- Excellent agreement for fine grid (within experimental error)
- Medium grid predicts slightly higher  $C_D$  after  $\alpha = 28^\circ$
- Coarse grid also performs well up to  $\alpha = 32^\circ$

## ⊗ Moment

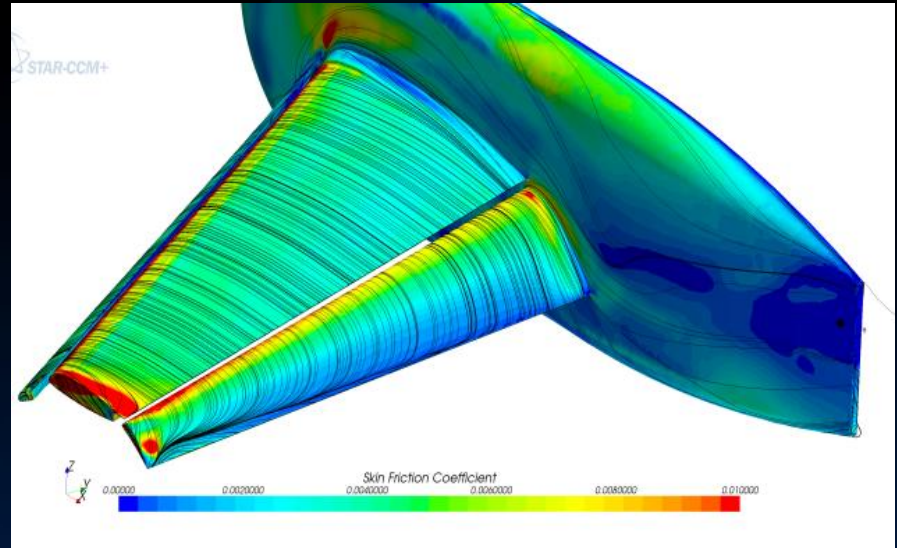
- $C_M$  showed the most deviation from experiments – harder to predict
- Performance improves with mesh refinement

# Effect of Transition Model

$\alpha = 13^\circ$

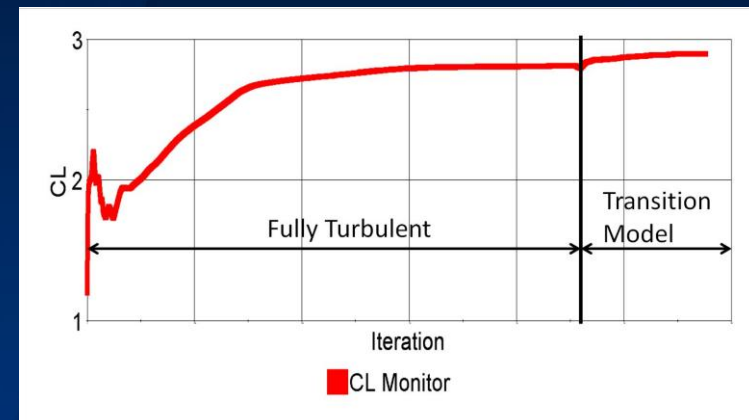


Transition Model



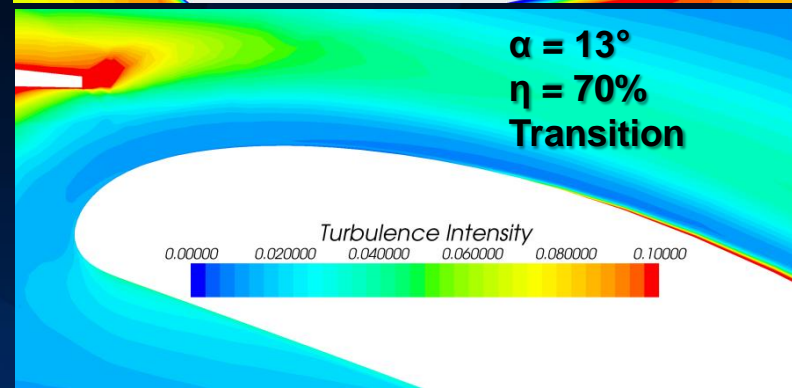
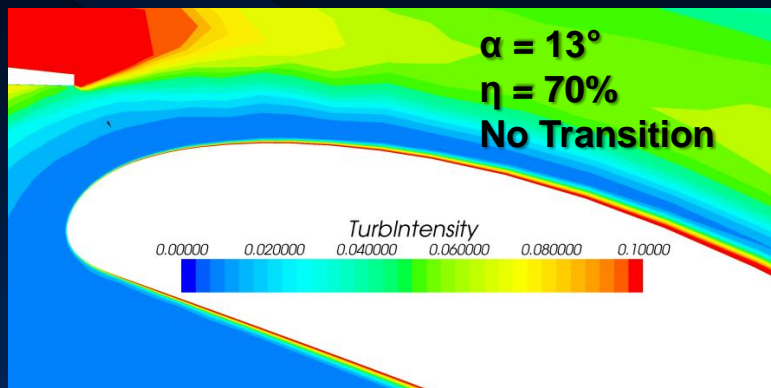
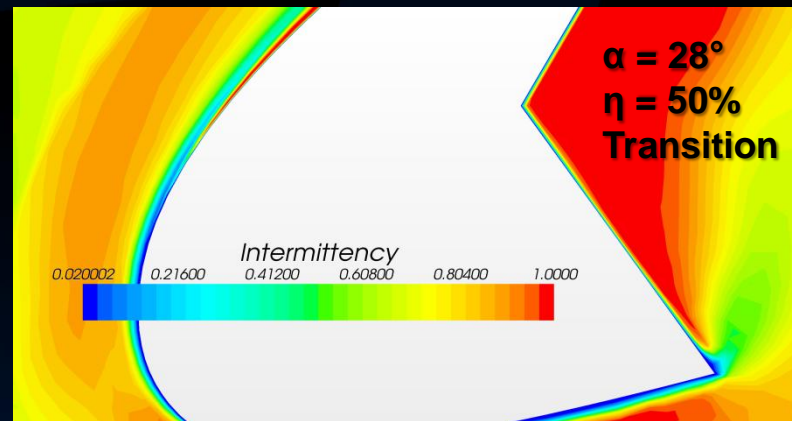
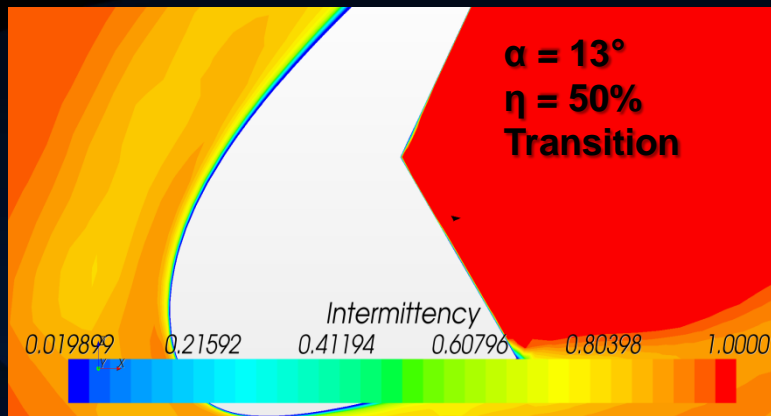
No Transition Model

- ⊗ Transition model increases lift coefficient
- ⊗ Transition model predicts larger flap separation
- ⊗ Flap side-of-body (SOB) separation bubble only predicted with transition model
  - Insufficient mesh resolution in this area for fully turbulent case
- ⊗ Skin friction coefficient on surface shows transition location



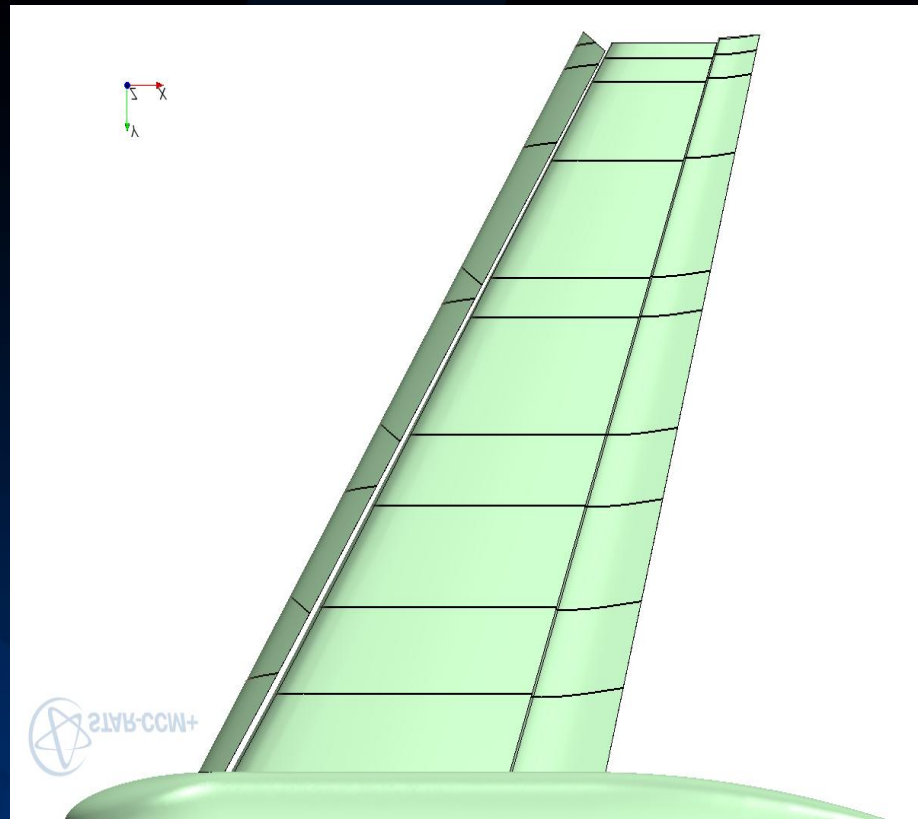
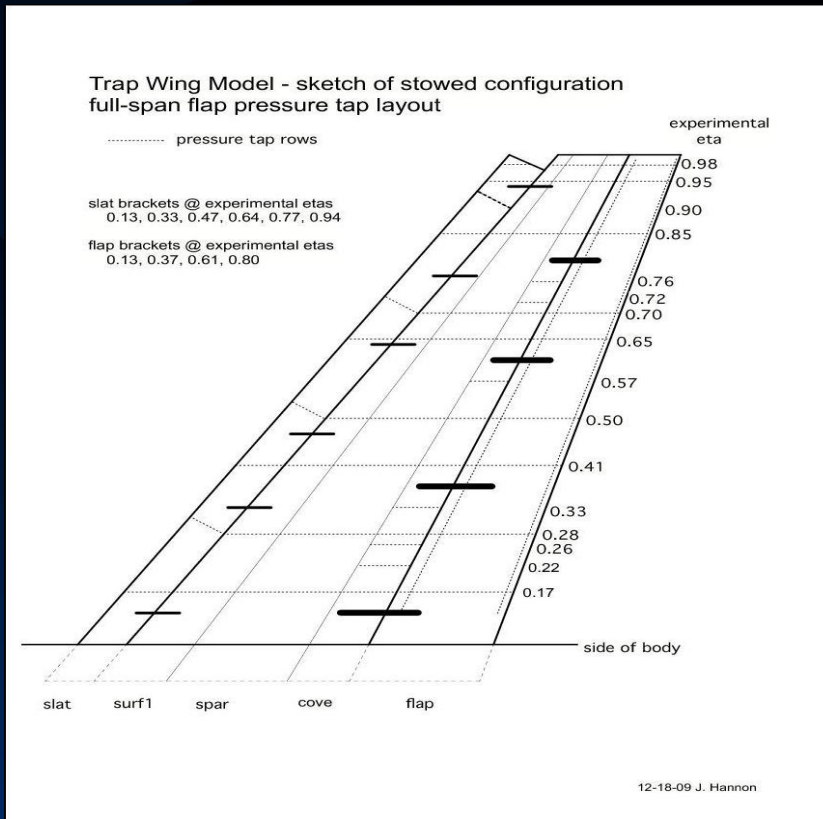


# Effect of Transition Model



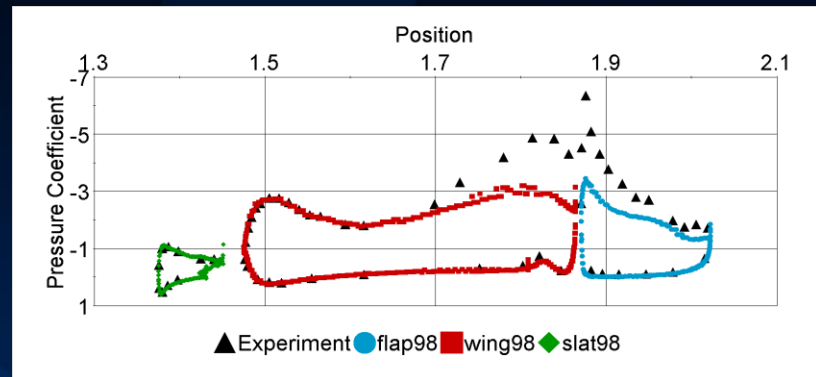
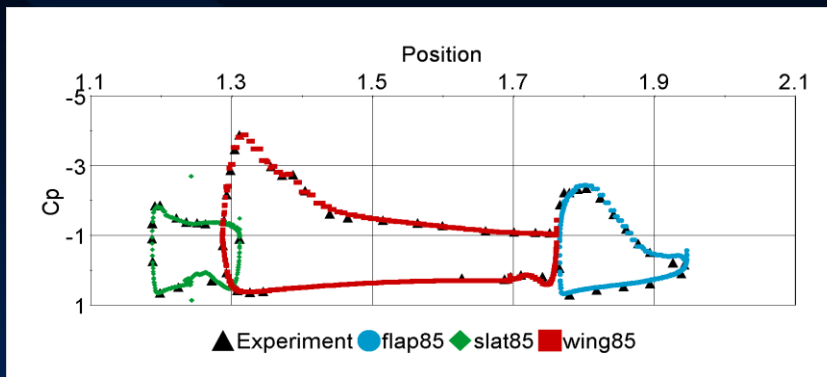
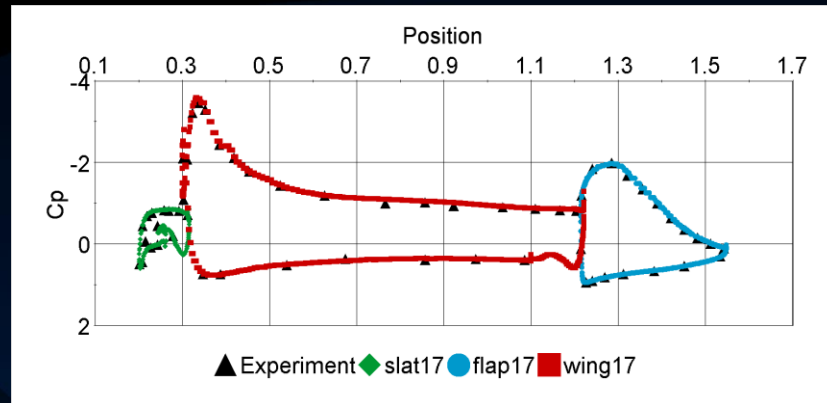
- ⊗ Intermittency ( $\gamma$ ) is used to identify flow transition
  - A value of 0 is laminar flow and 1 is turbulent flow
- ⊗ At  $13^\circ$ , flow over slat is laminar; at  $28^\circ$ , clear laminar-turbulent transition is seen from the  $\gamma$ - $Re_\theta$  model
- ⊗ Transition model captures transition on flap, yielding more accurate prediction of flap separation

# Surface Pressure Coefficients comparison



# Surface Pressure Coefficients – Medium Mesh

$\alpha = 13^\circ$



⊗ At  $\eta = 17, 50, \text{ and } 85\%$

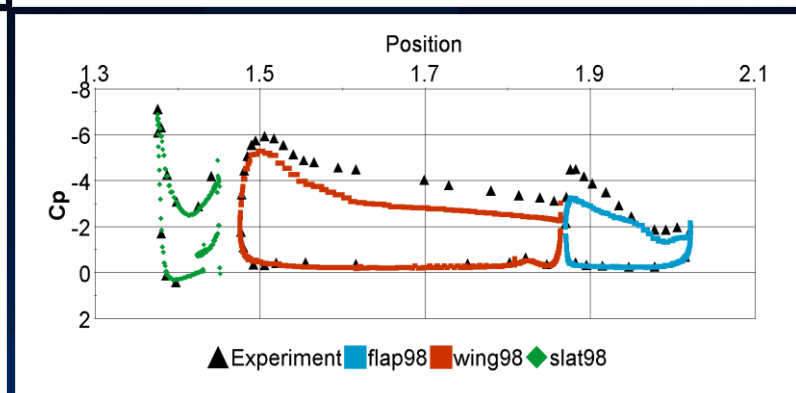
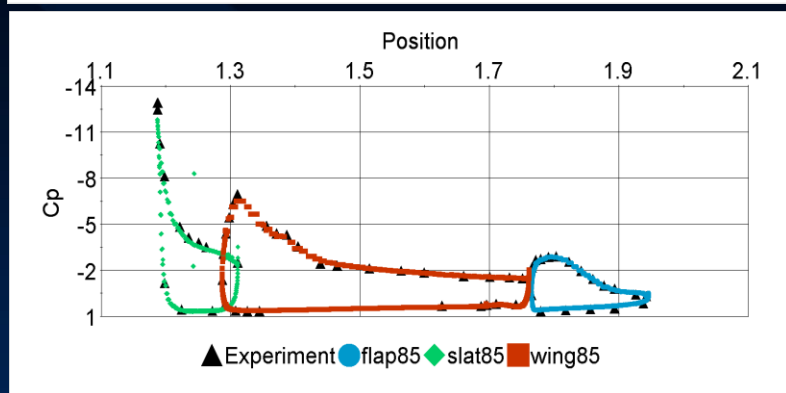
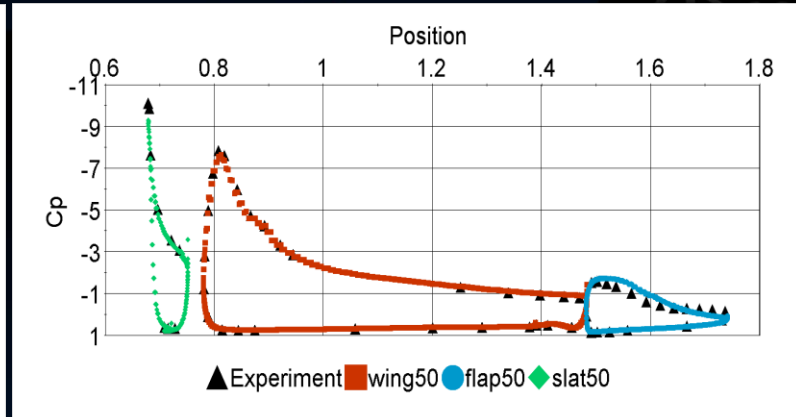
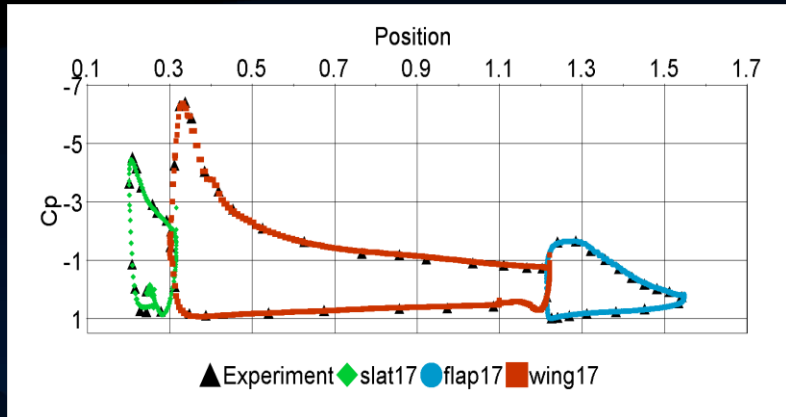
– Good agreement on slat, main wing, and flap

⊗ At  $\eta = 98\%$ , disparity is significant on main wing and flap

– Challenging to predict flap separation and tip vortex effects

# Surface Pressure Coefficients – Medium Mesh

$\alpha = 28^\circ$



⊗ At  $\eta = 17, 50, \text{ and } 85\%$

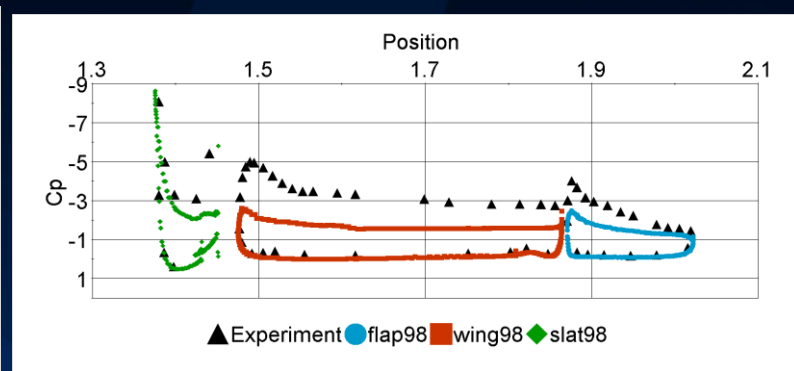
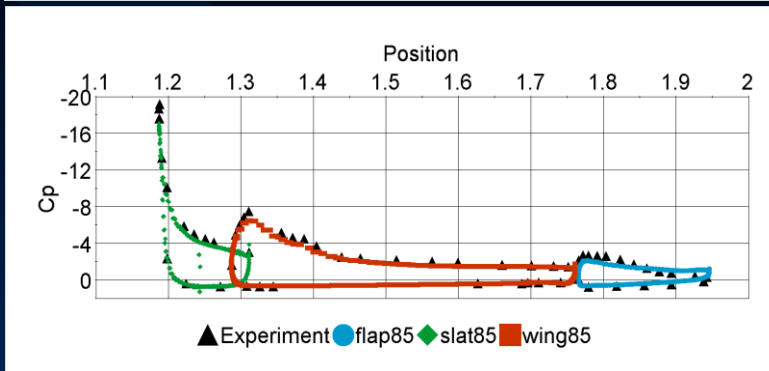
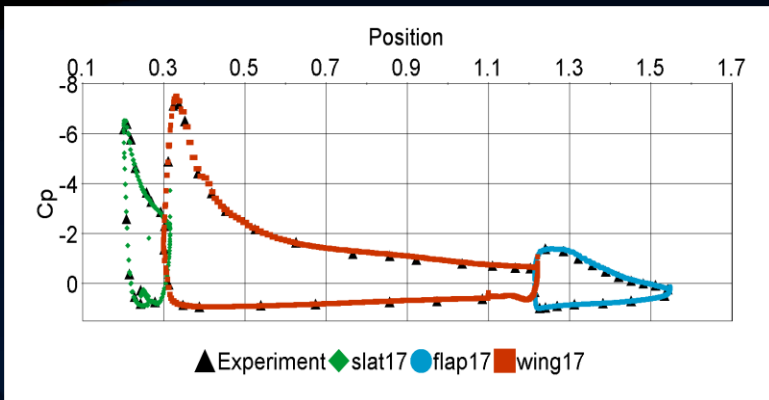
- Good agreement on slat, main wing, and flap
- Some discrepancy on flap suction surface noted at  $\eta = 50\%$

⊗ At  $\eta = 98\%$ , disparity is significant on main wing and flap

- Challenging to predict flap separation and tip vortex effects

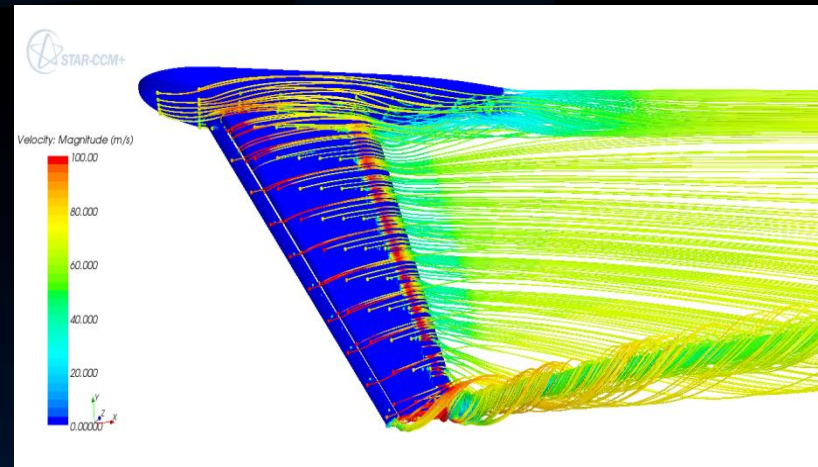
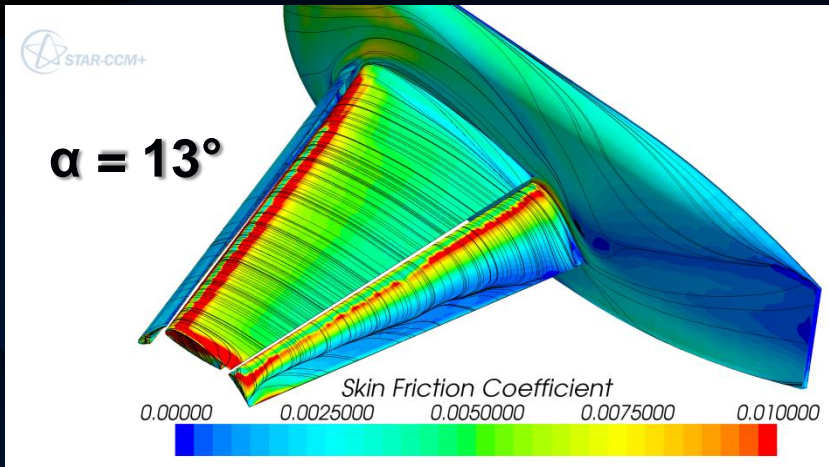
# Surface Pressure Coefficients – Medium Mesh

$\alpha = 34^\circ$



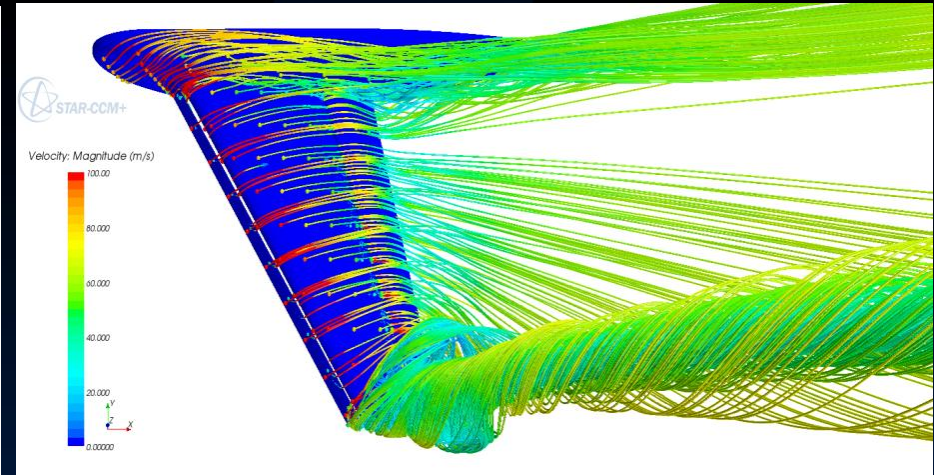
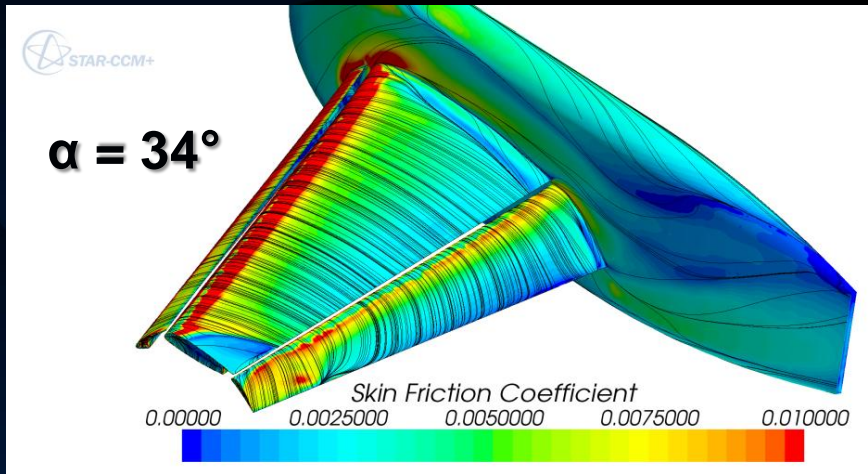
- ⊗ Even at post  $CL_{max}$  angle of  $34^\circ$ , surface pressure predictions are quite good until through 85% section for slat and main element
- ⊗ Significant over-prediction of flow separation near wing-tip at 98% section
- ⊗ Concentrated mesh refinement based on tip vortex structure will likely help here

# Surface Streamlines Comparison



- ⊗ At  $13^\circ$ , flap separation aft of mid-way nearly along entire span
- ⊗ Flap Side-of-body (SOB) separation bubble visible
- ⊗ Effective tip vortex is seen in the skin friction contours

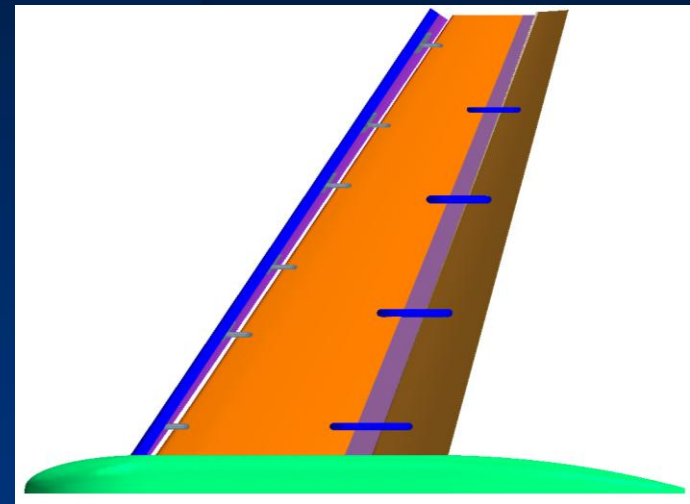
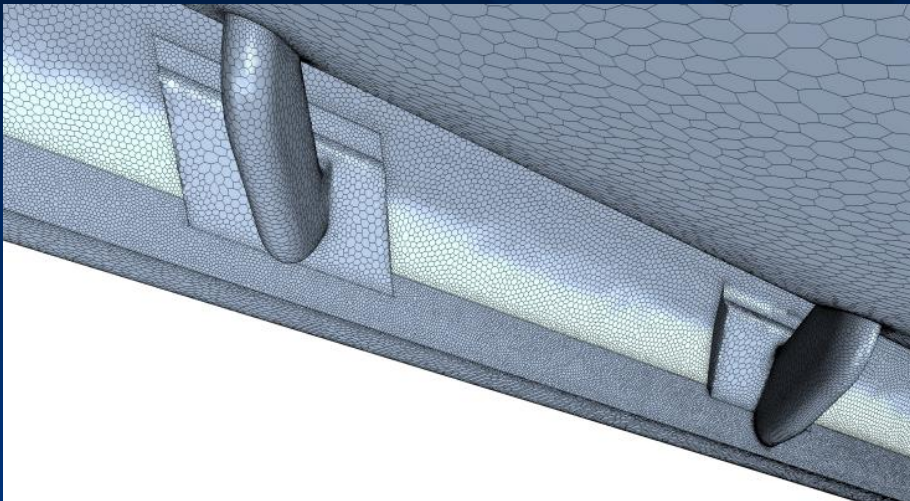
# Surface Streamlines Comparison



- ⊗ Flap separation delayed to TE
- ⊗ Large separation near the wing tip on the main element
- ⊗ Flap SOB separation disappears

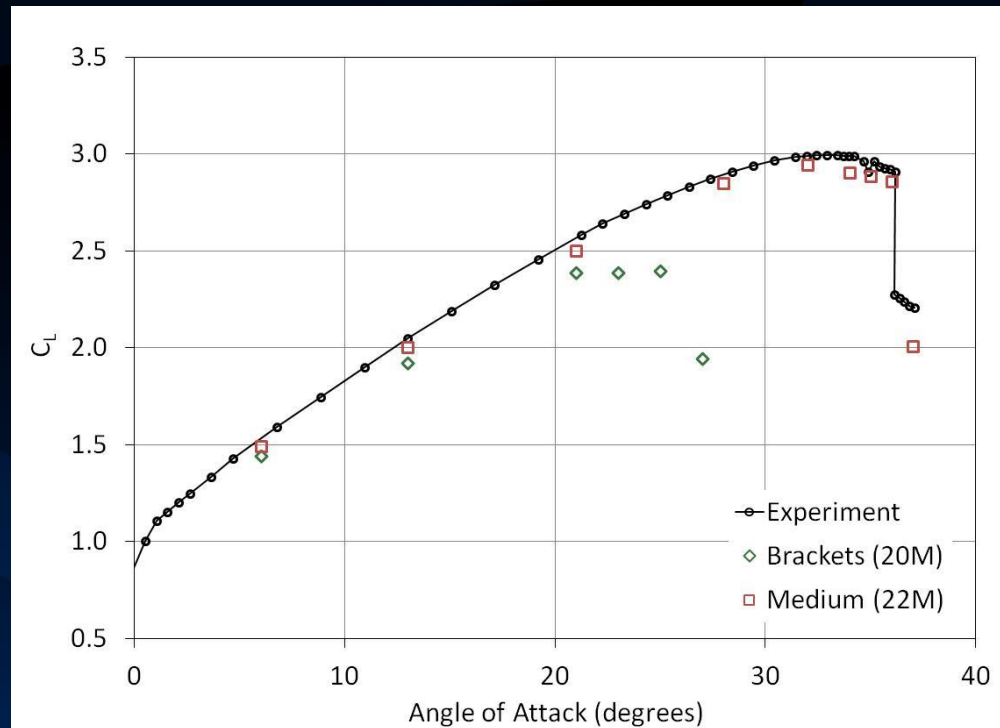
# Brackets Analysis

- ⊗ Config 1 with brackets at  $\alpha = 6^\circ, 13^\circ, 21^\circ, 23^\circ, 25^\circ, 27^\circ, 28^\circ$ 
  - Effect of flap and support brackets studied
  - 6 slat brackets and 4 flap brackets
  - Local flow separation
- ⊗ 22M medium mesh used as baseline mesh
- ⊗ No grid convergence study
- ⊗ Initial study to identify flow features and areas for focused refinement
- ⊗ All cases after  $21^\circ$  restarted from previous solution



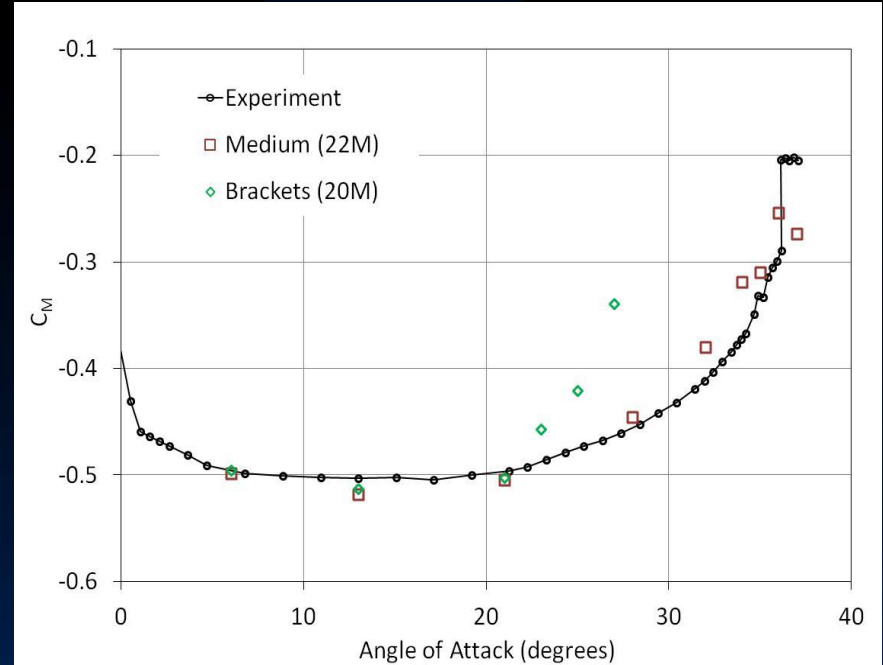
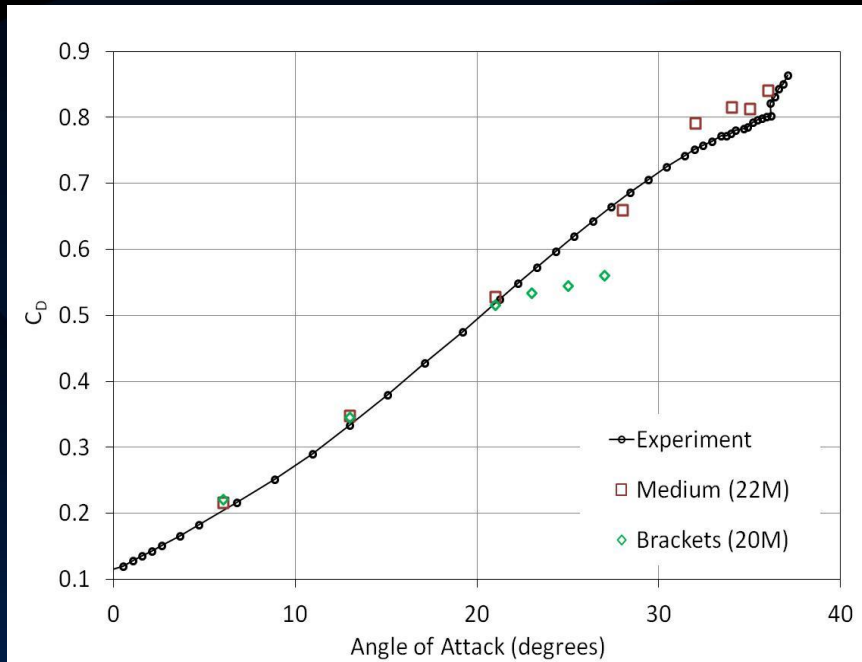


# Brackets Analysis – Lift Coefficient



- ⊗ CL is predicted lower compared to case without brackets at all angles of attack
  - Similar results from other participants
- ⊗ Early stall predicted after 21° resulting in loss of lift

# Brackets Analysis – Drag & Moment Coefficient



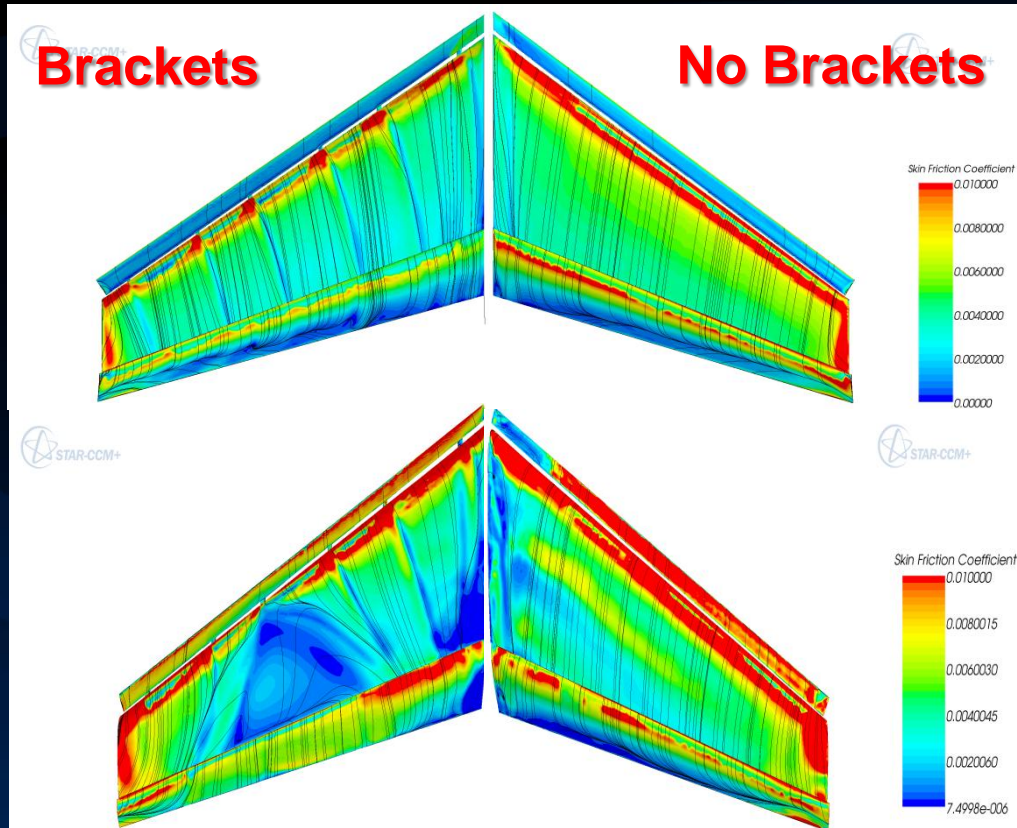
 Brackets have little effect on drag and pitching moment

– Until premature stall

# Brackets Analysis – Flow Visualization (Top view)



$\alpha = 13^\circ$



$\alpha = 28^\circ$

$\alpha = 13$

- Bracket wake affects transition on main element suction side
- Flap separation is delayed in local regions with brackets

$\alpha = 28$

- Massive flow separation occurs along bracket wake
- Early separation leading to stall – focused mesh refinement behind and around the brackets needed

# Conclusion



- ⊗ **General polyhedral mesh with predictive transition model yields good results**
  - Lift, drag & pitching moment
- ⊗ **Feasible methodology for production environment**
  - Mesh set-up time of 4 hrs (CAD to volume mesh)
- ⊗ **Brackets predict early stall**
  - Further investigation needed
  - Likely requires additional focused mesh refinement